Lifetime of the $4s^24p\ ^2P_{3/2}$ metastable level in galliumlike Mo^{11+}

Jianghui Bao, Yintao Wang, Jialin Liu, Jihui Chen, Liangyu Huang, Bingsheng Tu, Yunqing Fu, Chongyang Chen, Yaming Zou, and Ke Yao*

Shanghai EBIT laboratory, and Key Laboratory of Nuclear Physics and Ion-Beam Application (MOE), Institute of Modern Physics, Fudan University, Shanghai 200433, China

(Received 4 May 2023; accepted 30 May 2023; published 20 June 2023)

The lifetime of the galliumlike Mo^{11+} ion $4s^24p\ ^2P_{3/2}$ metastable level was measured at an electron-beam ion trap. The lifetime was inferred from the temporal behavior of its associated $4s^24p\ ^2P_{3/2} - {}^2P_{1/2}$ transition. Particular effort was devoted to reducing the systematic errors and the obtained lifetime value was $4.813(9)(^{+2}_{-5})$ (stat)(syst) ms. Most of the predictions without the electron anomalous magnetic moment correction are consistent with our measurement results. However, all the available, theoretical, effect-corrected results show an unexpected discrepancy with the measured results.

DOI: 10.1103/PhysRevA.107.062817

I. INTRODUCTION

Accurate measurements of lifetimes of atomic metastable levels, particularly in highly charged ions (HCIs), can be used to validate atomic structure calculations, including relativistic electron correlation and quantum electrodynamics (QED) effect calculations [1–5]. To date, precise experimental lifetime measurements with relative uncertainties of 0.5% or below have been reported (for a review, see Ref. [4]), which are immensely beneficial for exploring the QED effects in transition probabilities. For instance, the lifetime of the $2s^22p\ ^2P_{3/2}$ metastable level in Ar^{13+} [2] and that of the $3s^23p\ ^2P_{3/2}$ level in Fe^{13+} [3] have been determined with precisions in the order of 0.1%. Surprisingly, all the calculated line strengths [6–9], including the contribution from the anomalous magnetic moment (EAMM) (dominant QED effect), which accounts for approximately 0.46% of the transition rate, tend to predict shorter lifetimes than the measured results. Thus far, the reason for this discrepancy has not been explained. Therefore, more experimental studies on similar electron configurations (e.g., $4s^24p$) are required to address this ambiguity.

Forbidden transitions between the fine-structure levels of HCIs have also been proposed to develop ultraprecise optical clocks [10–12]. The proof of principle of an HCI optical clock has been demonstrated using the fine-structure $2s^22p\ ^2P_{3/2}$-$^2P_{1/2}$ transition in Ar^{13+} [13]. A total fractional uncertainty of 2.2×10^{-17} is obtained, which is comparable to those for the clocks in operation. However, for many other candidates, the clock-related atomic properties need to be determined experimentally and accurately in advance on the way toward the HCI clocks. Yu *et al.* [12] proposed the $4s^24p\ ^2P_{3/2}$ - $^2P_{1/2}$ magnetic dipole ($M1$) transition in galliumlike Mo^{11+} as the most suitable candidate for the ultraprecise optical clock. Nevertheless, to the best of our knowledge, there are no available measurements of the transition probability. The lifetime measurement can facilitate significant validation of the theory [12] and the natural linewidth also yields the parameters for evaluating atomic clock systematic uncertainties.

In this paper, we report a lifetime study of the galliumlike Mo^{11+} $4s^24p\ ^2P_{3/2}$ level at an electron-beam ion trap (EBIT). The measurement was performed by monitoring the temporal fluorescence decay from the $4s^24p\ ^2P_{3/2}$ - $^2P_{1/2}$ transition [$\lambda = 351.2088(24)$ nm in air [14]]. Possible systematic effects were investigated by examining the dependence of the decay curves on various experimental conditions. The lifetime of the $4s^24p\ ^2P_{3/2}$ level was determined at an uncertainty level below 0.3%.

II. EXPERIMENTAL METHOD

The measurement was carried out at the Shanghai EBIT laboratory using a newly developed 0.65 T room-temperature permanent magnet EBIT [15]. The EBIT has a discrete fourfold rotational symmetry magnetic structure, allowing for a wide field of view (see Fig. 1).

During the experiment, a volatile Mo molecular compound [molybdenum hexacarbonyl, $Mo(CO)_6$] is introduced into the trap center continuously from a direction perpendicular to the trap axis through a differentially pumped gas-injection system. The injection pressure is tuned using a micrometering valve. The EBIT provides a high-density monoenergetic electron beam, which efficiently ionizes the Mo beam and excites the ions. The ions are trapped radially by the electron-beam charge potential and the magnetic field, as well as axially by the appropriate electrostatic potentials applied to the outer drift tubes. To produce Mo^{11+} by electron-impact ionization, the electron-beam energy was set to 220 eV, which was sufficient to ionize Mo^{10+} (ionization potential: 209.3 eV [16,17]) but not Mo^{11+} (ionization potential: 230.3 eV [16,17]). The beam current was typically set to 1.5 mA to keep the elastic electron collision heating temperature as low as possible.

As illustrated in Fig. 1, the radiation emitted from the decay of the trapped excited ions was imaged using a lens onto

*keyao@fudan.edu.cn

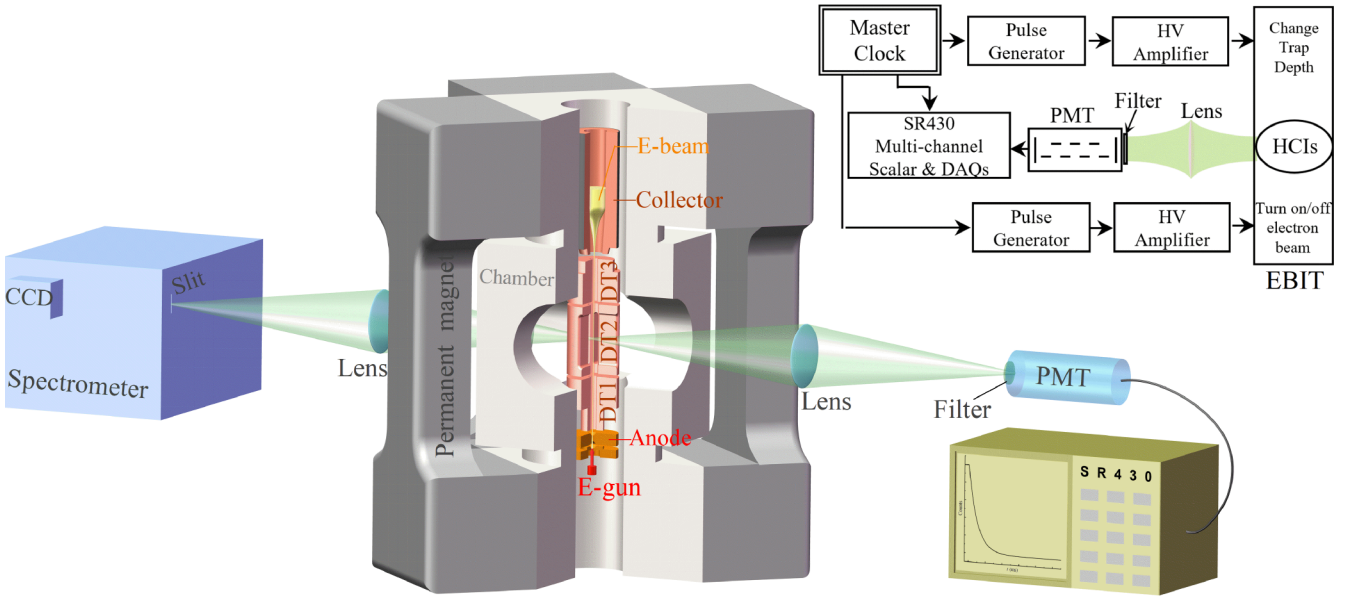

FIG. 1. Schematic illustration of the experimental setup. Fluorescent decay curves from the excited state are observed using a photomultiplier tube (PMT) coupled to the SR430 multichannel scaler. A high-resolution Czerny-Turner grating spectrometer equipped with a charge-coupled device was utilized to monitor the emission spectra simultaneously. The inset shows the block scheme of the data acquisition, as well as the detection systems used for the measurement.

a cooled photomultiplier tube (PMT, Hamamatsu R331-05). The output of the PMT was directly coupled to the input of a Stanford Research SR430 multichannel scaler, which had a built-in pulse discriminator. The scaler accumulates photon pulses in 40.96 μs bins. Prior to entering the PMT, the Mo^{11+} spectral line was selected by a narrow-band interference filter with a 10 nm bandwidth and a 60% transmission at 350 nm. Using the interference filter, stray photons of other wavelengths, which mainly come from the hot cathode, were excluded. Furthermore, to keep the background light counts due to the glow of the thermionic cathode as low as possible, the filament of the EBIT electron gun was driven at the lowest possible power required to attain the emission current. Additionally, a high-resolution Czerny-Turner grating spectrometer was employed to monitor the photons from the same trap volume.

The lifetime of the $4s^2 4p\ ^2P_{3/2}$ level in Mo^{11+} was measured by monitoring its spontaneous decay to $4s^2 4p\ ^2P_{1/2}$, for which the EBIT was operated in a cyclic mode with a period of 550 ms. The electron beam was turned on and off by applying 400 V and −100 V potentials to the anode electrode, respectively. In the measurements, the electron beam was turned on for 355 ms to ionize and excite the ions confined in the trap. Thereafter, the beam was turned off and the trap was maintained as a Penning trap in the magnetic trapping mode [18]. The emission decay was monitored during the beam-off period. The switching time of the electron beam (< 50 μs; much lower than the lifetime of the level of interest) was measured using a digital oscilloscope. However, even in the magnetic trapping mode, some of the ions gained sufficient energy through ion-ion collisions to overcome the potential barriers and subsequently evaporate from the trap. This ion loss reduced the experimental lifetime value. The Heidelberg EBIT group [1–3] reported that such ion losses could be well suppressed in a deep trap. Therefore, an eclectic trapping scheme, wherein not only the electron beam but also the trap depth is varied cyclically, was applied in this work. As shown in Fig. 2, during the ionization and excitation period (electron beam on), a shallow trap was chosen to increase the evaporative cooling rate, resulting in a low-temperature ion cloud. The trap was raised to a high potential 150 μs before turning off the electron beam. The deep potential was maintained for 200 ms until the electron beam was turned on again. Additionally, in each cycle, the accumulated ion cloud was purged from the trap to prevent the buildup of high-Z contaminants.

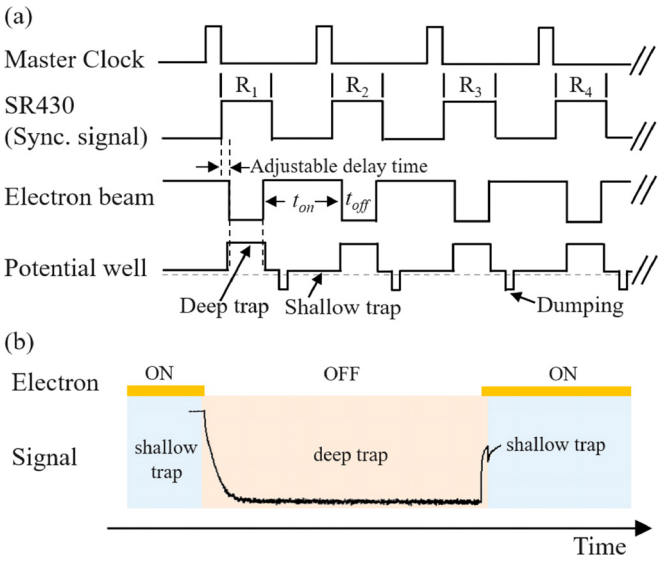

FIG. 2. Trapping scheme for the present lifetime measurement. (a) Timing diagram of the cyclic mode and (b) enlarged diagram of a single measurement with a period of 550 ms.

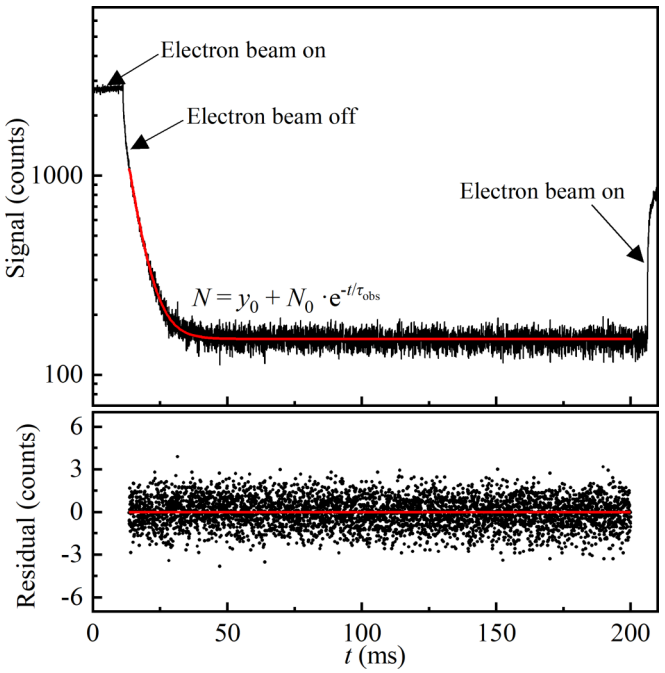

FIG. 3. Typical fluorescence decay curve (logarithmic scale) and its residual (normalized by $\sqrt{N}$, where N is the number of counts in each channel). The total acquisition time was approximately 48 h. The duration of each channel was 40.96 μs. The electron beam was turned off for 195 ms with a measurement cycle duration of 550 ms.

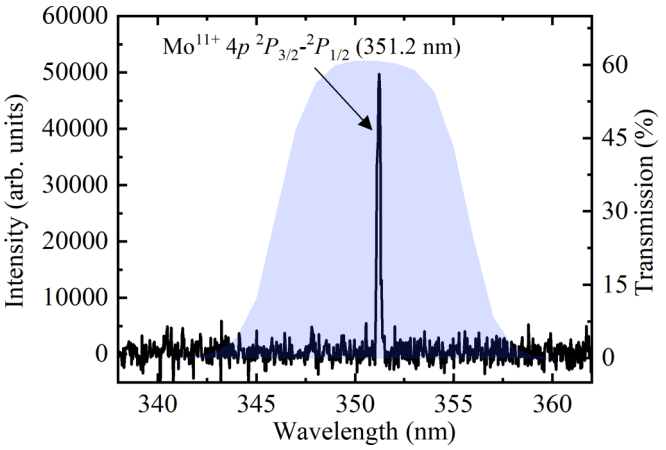

FIG. 4. Typical spectrum measured using the Czerny-Turner grating spectrometer when the electron beam was turned on. The shadow area presents the transmission rate of the filter (shown on the right axis). Only one spectral line from the Mo^{11+} $4s^2 4p\ ^2P_{3/2}$ - $^2P_{1/2}$ transition was detected.

III. DATA ANALYSIS AND THEORY

A. Experimental result analysis

A typical fluorescence decay curve is shown in Fig. 3. The decay curve could be fitted with a single exponential function, $N(t) = N_0 \exp(-t/\tau_{obs}) + y_0$, where N_0 is the initial intensity and τ_{obs} is the radiative decay constant of interest. y_0 represents a constant integrated background from the PMT dark counts and possibly from the stray light (from the hot electron gun cathode) falling into the narrow filter range. Notably, there is a fast nonexponential drop after the electron beam is switched off. To exclude the effect of the initial signal drop due to ion-cloud relaxation, the fitting was initiated at different times. After 2 ms, the fitted results became stable and exhibited only fluctuations within the statistical uncertainties. Further evaluations were conducted by varying the starting point from 2 to 5 ms after turning off the electron beam and no significant differences were found. Other higher-order exponential functions were also tested, but they failed to describe the data, indicating that there was no second decay component. Similarly, the tail of the decay curve was truncated to determine possible slow decay components. Again, no second decay component was retrieved.

The raw lifetime inferred from this single measurement, as shown in Fig. 3, is 4.808(19) ms. Thus far, only the fitting error from the fitting process in the single experiment was included, affording a relative accuracy of 0.4%. Here, the other possible systematic effects were not considered. Notably, contaminant lines, losses of ions (by charge-exchange recombination and ion escape), and state repopulation may affect the experimental results.

Figure 4 shows a typical spectrum recorded by a high-resolution grating spectrometer. Within the bandwidth of the filter (the purple area in Fig. 4), only Mo^{11+} $4s^2 4p\ ^2P_{3/2}$ - $^2P_{1/2}$ transition line is observed. No other blending lines are detected. Moreover, the transmittance is much less than 10^{-4} out of the filter bandpass. The decay curve cannot be affected by the contributions from any blending lines.

Measurements were also carried out at different gas injection pressures. No significant dependence of the measured lifetime on the gas pressures was found when the gas-injection pressure was below 2.3×10^{-7} torr. For the present lifetime experiment on Mo^{11+}, an injection pressure of 5.6×10^{-8} torr was employed.

The metastable level population loss due to the ion escape in the magnetic trapping mode will affect the measurements. The ion loss effect was studied using a sophisticated trapping potential scheme. As shown in Fig. 5(a), the measured lifetime for low axial trapping potentials (<100 V) was reduced (nearly 3% at 50 V), indicating that a fraction of the active ions overcome the axial potential barrier and escape from the trap. As the trapping potential increases, the lifetime reaches a plateau; thus the axial ion losses can be efficiently suppressed at deep trapping potentials higher than 100 V. However, the magnetic-field strength in the present EBIT is much weaker than that in a superconducting magnet EBIT. Ions produced at 8 V shallow trap are still hot enough to escape radially in the magnetic trapping mode due to its weak radial magnetic confinement, which makes the measured lifetime much shorter than the real one. The trapping potential of the shallow trap (electron beam on) was decreased stepwise to ensure sufficient evaporative cooling during ionization, affording low-temperature ions. Figure 5(b) shows the variation in the measured lifetime as a function of the drift tube potential during the beam-on period. The decay time increased as the trapping potential decreased from 8 V to 3 V, reaching an apparent constant value at trapping potentials less than 3 V. This shows that the ion losses in the

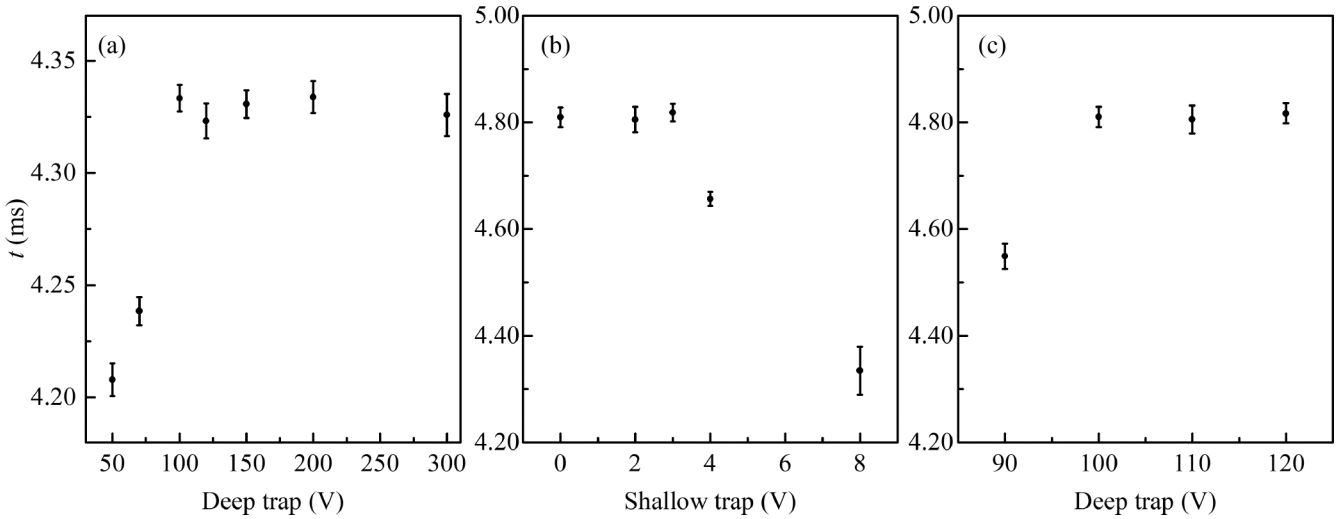

FIG. 5. Measured lifetimes vary with the deep trap depths (electron beam off) and the shallow trap depths (electron beam on). (a) Different deep trap depths at 8 V shallow trap, (b) different shallow trap depths at 100 V deep trap, and (c) different deep trap depths at 0 V shallow trap.

magnetic trapping mode can be well controlled. Furthermore, we conducted a set of experiments, wherein the deep trapping potentials were increased from 90 V to 120 V and the shallow trapping potential was maintained at 0 V [see Fig. 5(c)]. Similarly, at deep trapping potentials higher than 100 V, the escape rate was insignificant in comparison with the decay time. Generally, in our experiment, the ion escape can be considered to be negligible at relatively high deep trapping potentials and low shallow trapping potentials. The effective lifetime was determined by taking the weighted average of all the data points measured at the trap configurations, where the deep trapping potentials were higher than 100 V and the shallow trapping potentials less than 3 V. The lifetime of the $4s^24p\ ^2P_{3/2}$ level in Mo^{11+} obtained from the weighted average is 4.813 ± 0.009 ms, where 0.009 ms is the statistical uncertainty of all the measurements.

The charge-state distribution during the beam-off period might be affected by the charge exchange with neutral atoms or molecular compounds. In this work, a low-energy electron beam was employed and no Mo ions with charge states higher than Mo^{11+} were present in the trap. Therefore, the charge exchange only results in a loss of the metastable Mo^{11+} ions and would, therefore, make the measured value lower than the natural lifetime. The density of the neutral gas at the trap center was estimated to be approximately 2×10^6 cm^{-3} at the gas-injection pressure of 5.6×10^{-8} torr (below 7.6×10^{-11} torr in the EBIT chamber). According to the Müller-Salzborn formula [19,20], the single-electron charge-exchange cross section was estimated to be 4×10^{-14} cm^2 and the corresponding ion loss rate was approximately 0.1 s^{-1}. This value is an upper bound estimate, yielding a relative contribution of 0.05% to the transition probability.

The radiative cascade repopulation of the $4s^24p\ ^2P_{3/2}$ metastable level from higher levels might also introduce systematic errors into the measurement. Electric dipole ($E1$) transitions are too short lived to affect the measured lifetime in the millisecond range since they occur on the nanosecond timescale. Similar to the Al-like Fe^{13+} case studied in [3], only one known low-lying level ($4s4p4d\ ^4F_{9/2}$) decays via forbidden transitions and may contribute to the repopulation of the $4s^24p\ ^2P_{3/2}$ metastable level. The effect was evaluated by a collisional-radiative model calculation implemented in the FAC code [21]. The relativistic configuration interaction method was employed to calculate all the atomic data. The configurations included in our CR modeling are $4s^24p$, $4s^24d$, $4s^24f$, $4s4p^2$, $4s4p4d$, $4s4p4f$, $4p^3$, $4s^2nl$ ($n = 5, 6$), and $4s4pnl$ ($n = 5, 6$). In EBIT, radiative decay, as well as electron-impact excitation and deexcitation within the same ionization state, dominates the level population distribution [22–24]. All the electric and magnetic dipole, quadrupole, and octupole ($E1$, $E2$, $E3$, $M1$, $M2$, and $M3$) transitions among the above levels are considered in the present calculation. The result shows that nearly 99.7% of the Mo^{11+} ions are

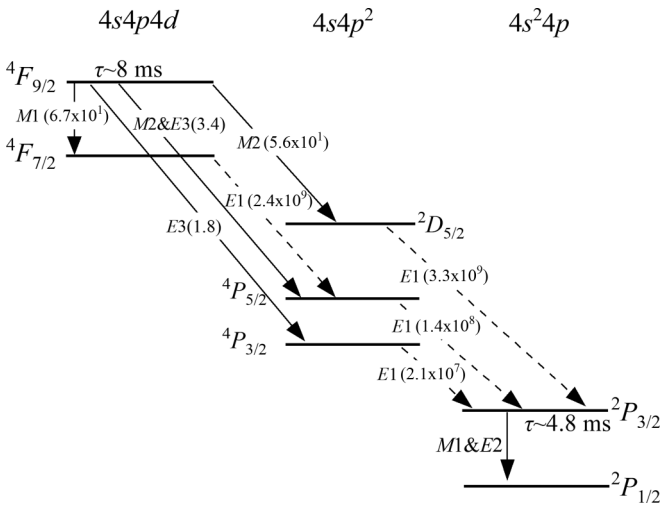

FIG. 6. Part of the level scheme of Mo^{11+}. The metastable $4s4p4d\ ^4F_{9/2}$ level has a calculated lifetime of approximately 8 ms. It has branching ratios to the $4s4p4d\ ^4F_{7/2}$, $4s4p^2\ ^2D_{5/2}$, $4s4p^2\ ^4P_{5/2}$, and $4s4p^2\ ^4P_{3/2}$ levels. These intermediate levels can decay into the $4s^24p\ ^2P_{3/2}$ level immediately via $E1$ transition. The numbers in parentheses are the calculated transition rates (in s^{-1}).

TABLE I. Estimation of experimental uncertainties.

Systematic effect	Relative contribution (%)
Statistics	±0.2
Charge exchange loss	+0.05
Ion escape	No
Cascade repopulation	−0.1
Dead time	No

populated in the $4s^2 4p\ ^2P_{1/2,3/2}$ levels. However, there are still 0.3% ions lying in the $4s4p4d\ ^4F_{9/2}$ metastable level with a lifetime of approximately 8 ms. As shown in Fig. 6, this metastable level can decay into the $4s^2 4p\ ^2P_{3/2}$ level by cascade repopulations via different transition channels, leading to a measured lifetime that is 0.1% longer than the real lifetime of the $4s^2 4p\ ^2P_{3/2}$ level.

The dead time of our data acquisition system mainly depended on the time resolution of the PMT and the multichannel scalar. It was measured to be approximately a few tens of nanoseconds. In this work, however, the maximum photon count rate (beam on) was less than 250 Hz. Therefore, the dead-time correction exerts a negligible effect on the experimental uncertainty.

The errors contributing significantly to the error budget are shown in Table I. The final experimental lifetime of the Mo^{11+} $4s^2 4p\ ^2P_{3/2}$ metastable level was determined to be $4.813(9)(^{+2}_{-5})$ (stat)(syst) ms.

B. Calculation and discussion

The $4s^2 4p\ ^2P_{3/2}$ metastable level can decay to the $4s^2 4p\ ^2P_{1/2}$ ground level through a magnetic dipole or electric quadrupole transition. Calculations show that the transition rate ratio A^{M1}/A^{E2} is more than 300. Therefore, the $M1$ decay dominates the process and the $E2$ decay is a small correction of the main decay channel. In general, the transition rate A^{M1} depends on the transition energy and the transition amplitude and it can be expressed as

$$A^{M1} = \frac{64\pi^4}{3h}\frac{1}{\lambda^3}\frac{S_{\rm if}}{2J_i+1}, \tag{1}$$

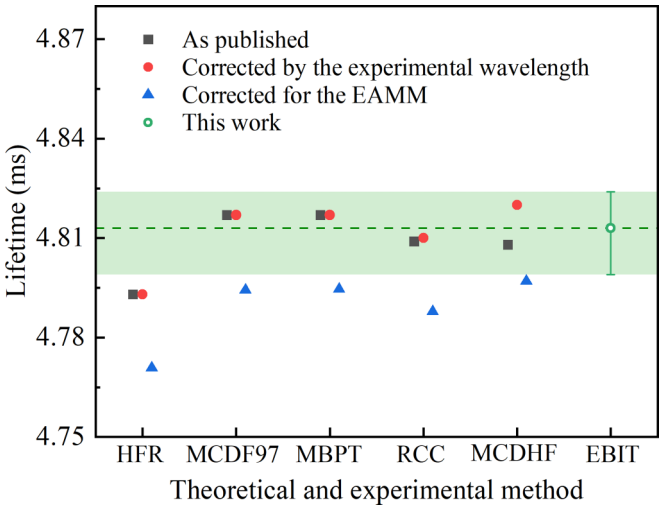

FIG. 7. Theoretical and experimental lifetimes of the Mo^{11+} $4s^2 4p\ ^2P_{3/2}$ metastable level. Corresponding values can be found in Table II. The theoretical values are from published works (HFR [25], MCDF97 [26], MBPT [27], and RCC [12]) and this work (MCDHF). The green translucent area shows the range of the experimental uncertainty.

where λ is the transition wavelength (in vacuum) and S_{if} is the line strength of the transition from upper level i to lower level f.

In this work, the MCDHF method based on the GRASP2K package [30] was employed to compute the rates of the $4s^2 4p\ ^2P_{3/2}$-$^2P_{3/2}$ transition of the Mo^{11+} ions. Electron correlations were included by allowing single and double excitations from the $\{4s, 4p\}$ valence subshells of the $\{4s^2 4p, 4s4p4d, 4p^3, 4p4d^2\}$ multireference (MR) sets and single excitations from the $\{2s, 2p, 3s, 3p, 3d\}$ core subshells of the same MR configurations to virtual active sets up to $n <= 8$, $l <= 6$. Breit interaction, vacuum polarization, and self-energy corrections were also considered in the subsequent configuration-interaction calculations. The calculated $M1$ line strength of the $4s^2 4p\ ^2P_{3/2}$-$^2P_{1/2}$ transition was 1.3303 (EAMM not included) and the corresponding wave number was 28486.9 cm^{-1}. In the calculation, it was also

TABLE II. Lifetime of the Mo^{11+} $4s^2 4p\ ^2P_{3/2}$ metastable level. Theoretical results from the relativistic Hartree-Fock self-consistent field method (HFR), multiconfiguration Dirac-Fock method (MCDF97), many-body perturbation theory (MBPT), relativistic coupled-cluster theory (RCC), and the present multiconfiguration Dirac-Hartree-Fock (MCDHF) calculation are presented. τ is the published value, $\tau_{\rm adj}$ is the adjusted lifetime using the precise experimental wavelength of 351.3092(24) nm, and $\tau_{\rm corr}$ is the corrected lifetime including the EAMM contribution. Notation $a(\pm b)$ corresponds to $a \times 10^{\pm b}$.

Method	A^{M1} (s^{-1})	A^{E2} (s^{-1})	λ (nm)	τ (ms)	$\tau_{\rm adj}$ (ms)	$\tau_{\rm corr}$ (ms)	$\tau_{\rm expt}$ (ms)
HFR [25]	2.08(+2)	6.19(−1)	351.32[a]	4.79	4.79	4.77	
MCDF97 [26]	2.07(+2)	5.98(−1)	351.32[a]	4.82	4.82	4.79	
MBPT [27]	2.07(+2)	5.87(−1)	351.32[a]	4.82	4.82	4.79	
RCC [12]	2.073(+2)	6.14(−1)	351.28[a]	4.809	4.810	4.788	
MCDHF (This work)	2.074(+2)	5.91(−1)	351.04	4.808	4.820	4.797	
Expt. (This work)							$4.813(9)(^{+2}_{-5})$ (stat)(syst)

[a]The available experimental wavelengths were obtained from published works. A value of 351.32 nm was measured by Curtis *et al.* [28], and 351.28 nm was determined by Reader *et al.* [29].

found that the line strength is not sensitive to the electron correlations.

To improve the precision of the calculations, we adjusted the calculated lifetime by employing the most precise experimental transition wavelength [351.3092(24) nm in vacuum [14]] and the theoretical line strength. Additionally, it is known that the main QED contribution to the $M1$ line strength could be derived in the lowest order by modifying the $M1$ operator of the atomic magnetic moment for the EAMM. The QED contribution can be included by redefining the line strength as $S_{if}^{\text{new}} = S_{if}(1 + 4\kappa_e)$, where $\kappa_e = \alpha/(2\pi)$ and $4\kappa_e$ accounts for 0.464% of the line strength [2,6,8]. The calculated results are listed in Table II.

The available theoretical lifetimes in the literature for the Mo^{11+} $4s^24p\ ^2P_{3/2}$ level using different methods are also listed in Table II and plotted in Fig. 7. The lifetimes modified using the most precise experimental wavelength and by incorporating the EAMM correction are also shown. Nearly all the theoretical lifetimes (black-filled squares and red-filled circles in Fig. 7) are within our experimental error margin. However, when the EAMM effect was considered, all the revised lifetimes (blue-filled triangles in Fig. 7) were slighter lower than the experimental results. Coincidentally, compared with the theoretical results [8,9,12], a similar discrepancy was also observed in a few other systems, e.g., the lifetimes of the $2s^22p\ ^2P_{3/2}$ metastable level in B-like Ar^{13+} [2] and the $3s^23p\ ^2P_{3/2}$ metastable level in Al-like Fe^{13+} [3]. These discrepancies have not been explained either by experiments or theories.

IV. SUMMARY AND OUTLOOK

The lifetime of the metastable $4s^24p\ ^2P_{3/2}$ level in galliumlike Mo^{11+} was first determined experimentally to be $4.813(9)(^{+2}_{-5})$ (stat)(syst) ms using an EBIT in the magnetic trapping mode. The lifetime precision of <0.3% achieved in this study is highly beneficial for improving the error budgets in various diagnostic applications and for benchmarking calculations. The theoretical results including the EAMM show a clear discrepancy with the present experimental results. More rigorous theoretical and experimental studies on similar ionic systems are required to address this ambiguity.

To achieve enhanced precision, we have started developing an ion trap to capture and store ions in the same charged state. The systematic effects caused by the mixture of charge states, the ion-cloud relaxation during the electron beam cutoff, and the stray light of the hot electron gun filament will be excluded. Additionally, as the electron collision excitation may induce cascade repopulation effects, we intend to apply laser excitation to perform level-selective lifetime measurements.

ACKNOWLEDGMENTS

This work is supported by the National Key R&D Program of China under Grant No. 2022YFA1602500 and by the National Natural Science Foundation of China through Grant No. 12274352.

[1] A. Lapierre, U. D. Jentschura, J. R. Crespo López-Urrutia, J. Braun, G. Brenner, H. Bruhns, D. Fischer, A. J. González Martínez, Z. Harman, W. R. Johnson, C. H. Keitel, V. Mironov, C. J. Osborne, G. Sikler, R. Soria Orts, V. Shabaev, H. Tawara, I. I. Tupitsyn, J. Ullrich, and A. Volotka, Relativistic Electron Correlation, Quantum Electrodynamics, and the Lifetime of the $1s^22s^22p^2\ P^o_{3/2}$ Level in Boronlike Argon, Phys. Rev. Lett. **95**, 183001 (2005).

[2] A. Lapierre, J. R. Crespo López-Urrutia, J. Braun, G. Brenner, H. Bruhns, D. Fischer, A. J. González Martínez, V. Mironov, C. Osborne, G. Sikler, R. Soria Orts, H. Tawara, J. Ullrich, V. M. Shabaev, I. I. Tupitsyn, and A. Volotka, Lifetime measurement of the Ar XIV $1s^22s^22p^2\ P^o_{3/2}$ metastable level at the Heidelberg electron-beam ion trap, Phys. Rev. A **73**, 052507 (2006).

[3] G. Brenner, J. R. Crespo López-Urrutia, Z. Harman, P. H. Mokler, and J. Ullrich, Lifetime determination of the Fe XIV $3s^23p\ ^2P^o_{3/2}$ metastable level, Phys. Rev. A **75**, 032504 (2007).

[4] E. Träbert, In pursuit of highly accurate atomic lifetime measurements of multiply charged ions, J. Phys. B: At., Mol., Opt. Phys. **43**, 074034 (2010).

[5] E. Träbert, Critical assessment of theoretical calculations of atomic structure and transition probabilities: An experimenter's view, Atoms **2**, 15 (2014).

[6] I. I. Tupitsyn, A. V. Volotka, D. A. Glazov, V. M. Shabaev, G. Plunien, J. R. Crespo López-Urrutia, A. Lapierre, and J. Ullrich, Magnetic-dipole transition probabilities in B-like and Be-like ions, Phys. Rev. A **72**, 062503 (2005).

[7] J. A. Santana, Y. Ishikawa, and E. Träbert, Multireference Møller-Plesset perturbation theory results on levels and transition rates in Al-like ions of iron group elements, Phys. Scr. **79**, 065301 (2009).

[8] C. F. Fischer, I. P. Grant, G. Gaigalas, and P. Rynkun, Lifetimes of some $2s^22p\ ^2P_{3/2}$ states from variational theory, Phys. Rev. A **93**, 022505 (2016).

[9] M. Bilal, A. V. Volotka, R. Beerwerth, and S. Fritzsche, Line strengths of QED-sensitive forbidden transitions in B-, Al-, F- and Cl-like ions, Phys. Rev. A **97**, 052506 (2018).

[10] V. I. Yudin, A. V. Taichenachev, and A. Derevianko, Magnetic-Dipole Transitions in Highly Charged Ions as a Basis of Ultraprecise Optical Clocks, Phys. Rev. Lett. **113**, 233003 (2014).

[11] D. K. Nandy and B. K. Sahoo, Highly charged W^{13+}, Ir^{16+}, and Pt^{17+} ions as promising optical clock candidates for probing variations of the fine-structure constant, Phys. Rev. A **94**, 032504 (2016).

[12] Y.-M. Yu and B. K. Sahoo, Investigating ground-state fine-structure properties to explore suitability of boronlike S^{11+} – K^{14+} and galliumlike Nb^{10+} – Ru^{13+} ions as possible atomic clocks, Phys. Rev. A **99**, 022513 (2019).

[13] S. A. King, L. J. Spieß, P. Micke, A. Wilzewski, T. Leopold, E. Benkler, R. Lange, N. Huntemann, A. Surzhykov, V. A. Yerokhin *et al.*, An optical atomic clock based on a highly charged ion, Nature (London) **611**, 43 (2022).

[14] Y. Li, Y. Wang, J. Fan, R. Si, J. Li, M. Zhang, L. Huang, J. Xiao, Y. Zou, B. Wei, and K. Yao, Precise wavelength determination of the $4s^2 4p\ ^2P_{3/2}$ - $^2P_{1/2}$ transition in Mo^{11+} and Ru^{13+} ions, J. Phys. B: At., Mol., Opt. Phys. **54**, 235001 (2021).

[15] L. Y. Huang *et al.* (unpublished).

[16] A. Kramida, Yu. Ralchenko, J. Reader, and NIST ASD Team, NIST Atomic Spectra Database (ver. 5.10) [online]. Available at https://physics.nist.gov/asd (National Institute of Standards and Technology, Gaithersburg, MD, 2022).

[17] J. Sugarand A. Musgrove, Energy levels of molybdenum, Mo I through Mo XLII, J. Phys. Chem. Ref. Data **17**, 155 (1988).

[18] P. Beiersdorfer, L. Schweikhard, J. C. López-Urrutia, and K. Widmann, The magnetic trapping mode of an electron beam ion trap: New opportunities for highly charged ion research, Rev. Sci. Instrum. **67**, 3818 (1996).

[19] B. M. Penetrante, J. N. Bardsley, D. DeWitt, M. Clark, and D. Schneider, Evolution of ion-charge-state distributions in an electron-beam ion trap, Phys. Rev. A **43**, 4861 (1991).

[20] I. V. Kalagin, D. Küchler, V. P. Ovsyannikov, and G. Zschornack, Modelling of ion accumulation processes in EBIS and EBIT, Plasma Sources Sci. Technol. **7**, 441 (1998).

[21] M. F. Gu, The flexible atomic code, Can. J. Phys. **86**, 675 (2008).

[22] R. Doronand U. Feldman, Visible and near UV $M1$ transitions within N-shell ground configurations of heavy ions predicted to be bright in low-density plasmas, Phys. Scr. **64**, 319 (2001).

[23] V. Jonauskas, Š. Masys, A. Kynienė, and G. Gaigalas, Cascade emission in electron beam ion trap plasma, J. Quant. Spectrosc. Radiat. Transfer **127**, 64 (2013).

[24] Z. He, J. Meng, Y. Li, F. Jia, N. Khan, B. Niu, L. Huang, Z. Hu, J. Li, J. Wang, Y. Zou, B. Wei, and K. Yao, Magnetic-dipole lines in Fe-like and Mn-like molybdenum ions, J. Quant. Spectrosc. Radiat. Transfer **288**, 108276 (2022).

[25] E. Biémontand J. Hansen, Calculations of transition probabilities for forbidden lines in $3p^n$ and $4p^n$ configurations, Nucl. Instrum. Methods Phys. Res., B **23**, 274 (1987).

[26] M. A. Ali, Fine-structure splitting and magnetic dipole and electric quadrupole transition probabilities between the ground levels of Ga-like ions, Phys. Scr. **55**, 159 (1997).

[27] U. Safronova, T. Cowan, and M. Safronova, Relativistic many-body calculations of energies, $E2$, and $M1$ transition rates of $4s^2 4p$ states in Ga-like ions, Phys. Lett. A **348**, 293 (2006).

[28] L. J. Curtis, J. Reader, S. Goldsmith, B. Denne, and E. Hinnov, $4s^2 4p\ ^2P$ intervals in the Ga isoelectronic sequence from Rb^{6+} to In^{18+}, Phys. Rev. A **29**, 2248 (1984).

[29] J. Reader, N. Acquista, and S. Goldsmith, $4s^2 4p - 4s4p^2$ and $4s^2 4p - 4s^2 5s$ transitions of galliumlike ions from Rb VII to In XIX, J. Opt. Soc. Am. B **3**, 874 (1986).

[30] P. Jönsson, G. Gaigalas, J. Bieroń, C. F. Fischer, and I. Grant, New version: Grasp2K relativistic atomic structure package, Comput. Phys. Commun. **184**, 2197 (2013).